Calcium filled skutterudites $Ca_xCo_4Sb_{12}$: effect of the computational approach on the *ab-initio* modeled electronic transport properties

2008 J. Phys.: Conf. Ser. 117 012010

(http://iopscience.iop.org/1742-6596/117/1/012010)

Journal of Physics: Conference Series **117** (2008) 012010 doi:10.1088/1742-6596/117/1/012010

Calcium filled skutterudites $Ca_xCo_4Sb_{12}$: effect of the computational approach on the *ab-initio* modeled electronic transport properties.

Simone Cenedese[1], Luca Bertini[2] and Carlo Gatti[1]

[1] Istituto di Scienze e Tecnologie Molecolari (CNR-ISTM), Via C. Golgi 19, 20133 Milano, Italy
[2] Dipartimento di Biotecnologie e Bioscienze, Università degli Studi di Milano Bicocca, Piazza della Scienza 2, 20156 Milano, Italy

E-mail: c.gatti@istm.cnr.it

Abstract. Fully filled $CaCo_4Sb_{12}$ system is selected as a test case for probing how the *ab-initio* modeled electronic transport properties are affected by the computational level. The periodic wave functions for the various adopted models are calculated by means of the Density Functional Theory (DFT) approach using local gaussian atomic basis sets, while the relevant electronic transport properties are obtained from the band structure using the semi-classical Boltzmann transport theory. This two-step computational procedure is tested against the atomic basis set quality, the band structure adopted in the frozen band approach and the DFT functional form. From this extensive test, a reliable computational level for $CaCo_4Sb_{12}$ is identified and the experimental findings on the Ca-filled systems are discussed in the light of, and compared with, the results from computations.

1. Introduction

Optimizing the thermoelectric (TE) properties of a material requires to maximize its figure of merit $Z \cdot T = T \cdot S^2 \sigma (\kappa_e + \kappa_L)^{-1}$, where S is the Seebeck coefficient, σ the electric conductivity, and κ_e and κ_L are the electronic and lattice contributions to the total thermal conductivity. For instance, given a semiconductor as a starting point of this optimisation, one can generally improve $Z \cdot T$ through doping and then maximize $Z \cdot T$ against the dopant atom content.

Recently [1-4], the *ab-initio* modeling of the material's electronic structure has proved useful in this optimization process for its ability of describing and predicting the effects that the material's modifications have on its electronic transport properties (S, σ and κ_e). These quantities may be evaluated from the system's periodic wave function and band structure using Boltzmann semiclassical transport theory [5] and without resorting to any empirical information.

This paper deals with the *ab-initio* determination of the $Ca_xCo_4Sb_{12}$ filled skutterudite system, whose TE properties have recently been studied experimentally by Puyet *et al*. [6-7]. Aim of this work is to assess how sensitive are the calculated properties with respect to the adopted computational level, so as to select a suitable computational model for $Ca_xCo_4Sb_{12}$ among several possible, and to generally gain insight on the reliability of the *ab-initio* approach for the TE materials modelling.

2. Theoretical and computationals details

2.1. Electronic structure calculation.
Fully periodic DFT *ab-initio* calculations were performed using CRYSTAL03 code [8]. Hay-Wadt pseudopotentials (PP) [9], with small Core PP for Co and Ca atoms (17 and 10 active electrons, respectively) and Large Core for Sb atom (5 active electrons) were adopted. The basis sets used in this work are of double-ζ and triple-ζ quality and the procedures followed for tuning them are detailed in the next section. All calculations were carried out in the Im-3 space group (unit) cell, with 4 Co atoms at the *8c* and 12 Sb atoms at the *24g* special positions. For each system the structural parameters (cell parameter and the free fractional coordinates of Sb atoms) were optimized. The total electron density ρ(**r**) has been investigated within the Quantum Theory of Atoms in Molecules (QTAIM) [10] approach using the TOPOND-98 package [11], which implements QTAIM to periodic systems.

2.2. Electronic transport properties (ETPs) calculation.
We estimated the ETPs (the Seebeck coefficient **S**, the electrical conductivity **σ** and the electronic contribution to the thermal conductivity, $\boldsymbol{\kappa}_e$) using the ELTRAP [12] code which is interfaced to the CRYSTAL98 calculation package [13] and which implements the semi-classical Boltzmann transport theory in its monoelectronic formulation [1], within the constant relaxation time approximation.

The ETPs are second-rank tensors and they are derived from the Onsager coefficients $\mathbf{L}_i$,

$$\mathbf{L}_i = 2\sum_n \int_{1BZ} \tau_n(\mathbf{k},T) v_n^2(\mathbf{k}) \left(E_n(\mathbf{k}) - \mu\right)^i \left(-\frac{\partial f_0}{\partial \varepsilon}\right)_{\varepsilon = E_n(\mathbf{k})} d\mathbf{k}, \quad i = 0-2 \tag{1}$$

The integral in the **k**-space is over the first Brillouin zone (1BZ), $\tau_n(\mathbf{k},T)$ is the relaxation time, $E_n(\mathbf{k})$ and $\mathbf{v}_n(\mathbf{k}) = (1/\hbar)\partial E_n(\mathbf{k})/\partial \mathbf{k}$ are, respectively, the n-th band energy and velocity as a function of **k**, and μ is the chemical potential. For any given temperature T, μ is derived from the expression of the Fermi-Dirac distribution f_0,

$$N_e N_{\mathbf{k}} = \sum_{n,\mathbf{k}} 2 f_0 = \sum_{n,\mathbf{k}} \frac{2}{1 + e^{[E_n(\mathbf{k}) - \mu]/(k_B T)}} \tag{2}$$

where N_e and $N_{\mathbf{k}}$ are the number of electrons in the cell and the number of **k** points sampling each band, respectively. By assuming a constant relaxation time τ, independent of **k**, n and T, the three ETPs **σ**, **S** and $\boldsymbol{\kappa}_e$ are easily calculated as [5]

$$\boldsymbol{\sigma} = e^2 \tau \mathbf{L}_0 \quad ; \quad \mathbf{S} = \frac{1}{eT}\mathbf{L}_0^{-1}\mathbf{L}_1 \quad ; \quad \boldsymbol{\kappa}_e = \frac{\tau}{T}\left(\mathbf{L}_2 - \mathbf{L}_1\mathbf{L}_0^{-1}\mathbf{L}_1\right)$$

In the results section, the isotropic part of the electronic transport properties tensors, given as 1/3 of their traces, are reported. The integrals [equation (1)] are evaluated numerically by sampling $E_n(\mathbf{k})$, using an equally spaced cubic grid with a total of $N_{\mathbf{k}} = 40^3$ points per band [14] and 16 bands around the Fermi level (8 below and 8 above). The constant relaxation time was taken equal to 10^{-14} s.

It must be noted that in $Ca_xCo_4Sb_{12}$ the maximal solubility of the filler atom is about x=0.2 [6]. ETPs have thus been computed within the frozen band approach. Systems with x less than one can be simulated using the x=1, x=0.5 or x=0 reference band structures which, in our case, means considering $CaCo_4Sb_{12}$, 2×1 supercell $Ca_{0.5}Co_4Sb_{12}$ or Co_4Sb_{12} systems. The number of electrons N_e is then properly adjusted to match the value of x of the doped system under investigation [decreased by ΔN_e=

2(1-x) and $\Delta N_e = 2(0.5-x)$, respectively, for the first two reference systems, and augmented by $\Delta N_e = 2x$ for the latter] and the Fermi level (chemical potential) is recalculated according to equation (2).

As in [4] and in [15], the optimal doping level was evaluated by maximizing the power factor $S^2\sigma$. This approach permits to locate the position of the most favourable doping at a given T, in the hypothetical case of $\kappa_L >> \kappa_e$. As in our previous paper [3], we also used the electronic figure of merit $Z_e \cdot T = T \cdot (S^2\sigma/\kappa_e)$ as an ideal ($\kappa_L = 0$) upper bound to the total figure of merit $Z \cdot T$. The electronic figure of merit has the advantage of being formally τ independent, although it is only so if the two relaxation times, that for the electric current, τ_σ, and that for the thermal current, τ_κ, are equal to each other. Since this is generally far to be true, $Z_e \cdot T$ serves mainly to attain a rough estimate of $Z \cdot T$ once the optimal doping level has been obtained by the maximal $S^2\sigma$ criterion.

3. Tuning the computational model

In the first paragraph of this section, the strategy adopted to select the atomic basis sets for calculating the $CaCo_4Sb_{12}$ electronic structure is illustrated and the main differences in the electronic structure upon adoption of different basis set are highlighted. The dependence of the computed electronic transport properties on the band structure adopted as a reference (single cell $CaCo_4Sb_{12}$, 2×1 supercell $Ca_{0.5}Co_4Sb_{12}$ and unfilled Co_4Sb_{12}) is discussed in the second paragraph. Finally, we show how the calculated ETPs are affected by the nature of the DFT functional.

3.1. Basis set

The choice of the optimal atomic basis set (BS) is a delicate task when *ab-initio* periodical calculations based on local gaussian BSs are performed. The BS set must be flexible enough, properly adapted to the crystalline environment and reasonably compact so as to yield satisfactory results, while not being too CPU time consuming. This is a crucial point since the band structure sampling [1] used in the calculation of the ETPs has an high computational cost, about two order of magnitude larger than for the SCF step. The tuning of the Ca, Co and Sb atomic BSs for $CaCo_4Sb_{12}$, using Becke3 [16] and PW91 [17] correlation potentials (B3PW91) for the DFT functional, is detailed below. The contraction schemes of the different basis sets considered are listed in table 1.

Table 1. Contraction schemes of the adopted basis sets

	Ca	Co	Sb
OBS[a]	10S,5P ; 3S(3,4,1),3P(3,1,1)	10S,5P,5D	3S,3P
PBS[b]	8S,4P ; 3S(3,3,1),2P(3,1)	8S,4P,5D	3S,3P
TZ	4S(4,2,1,1),3P(2,1,1)	4S(4,2,1,1),3P(2,1,1),3D(3,1,1)	3S(1,1,1),3P(1,1,1)
DZ1	3S(3,3,1),2P(3,1)	3S(4,3,1),2P(3,1),2D(4,1)	2S(2,1),2P(2,1)
DZ1d	3S(3,3,1),2P(3,1),1D(1)	3S(4,3,1),2P(3,1),2D(4,1)	2S(2,1),2P(2,1)
DZ2	2S(3,3),1P(3),1SP(1)	2S(4,3),1P(3), 2D(4,1),1SP(1)	1S(2),1P(2),1SP(1)
DZ2d	2S(3,3),1P(3),1SP(1),1D(1)	2S(4,3),1P(3), 2D(4,1),1SP(1)	1S(2),1P(2),1SP(1)

[a] First OBS entry for Ca refers to Hay-Wadt PP [9], while the second refers to its double-ζ contraction [21].
[b] The first (second) PBS entry for Ca is derived from the first (second) OBS for Ca.

Starting from the Original atomic gaussian minimal Basis Sets (OBS) [9] relative to these PP we generate the Periodic atomic Basis Sets (PBS) by removing the outermost *ns* and *np* gaussian functions [18] in the original primitive set before contraction. From the PBS, new triple-ζ (TZ) and double-ζ (DZ1) contractions were generated for Co and Sb, with contraction coefficients variationally determined at the atomic level [19]. The TZ contraction scheme for Ca has been similarly generated.

The DZ1 contraction scheme for Ca has a slightly different origin [20] with the reference OBS being itself a double-ζ modification [21] of the original Hay-Wadt PP. The DZ2 basis set is obtained from DZ1 basis by imposing the *s*=*p* constraint on the most diffuse shell of each atom. A single gaussian *d* shell (exponent 0.15) was added, for the Ca atom, to the DZ1 and DZ2 basis sets, yielding

the DZ1d and DZ2d basis sets. The electronic structure and the ETPs of $CaCo_4Sb_{12}$ were evaluated for the DZ1, DZ2, DZ1d and DZ2d basis sets at the corresponding optimized cell structures. All properties are listed in table 2.

$CaCo_4Sb_{12}$ reveals to be an heavily *n*-doped semiconductor in all cases, as portrayed by the total density of states (DOS) in figure 1 for the B3PW91/DZ2 model. The features of the $CaCo_4Sb_{12}$ band structure are explained with reference to that of the unfilled Co_4Sb_{12} system, discussed by Anno *et al*. [22]. Co_4Sb_{12} is a narrow band gap semiconductor, with the highest occupied (HOB) and first unoccupied (FUB) bands basically due to suitable combinations of bonding and antibonding Sb_4 π orbitals and of Co *d* orbitals of E_g symmetry [23]. Below the Fermi Level (FL) the bands are dominated by the Co *d* contributions, while above this level, the bands consist mainly of contributions from the Sb π orbitals. By integrating the DOS up to the FL, we obtain a Co *d* population of 8.37 e^-. This *d* population increase with respect to that of the Co metal (7.50 e^-) agrees with the picture found by Kurmaev *et al*. [24] for Co_4Sb_{12} and by Partik *et al*. [25] for Co_4P_{12}.

Table 2. The effect of the basis set. Cell parameter *a* and the free fractional coordinates, *y* and *z*, of Sb atoms. Total energy (E) in hartree; Fermi level (FL) in eV; band gap (E_g) energy in eV; q(Ca) is the QTAIM atomic net charge for Ca; *x* is the optimal filling fraction according to the power factor $S^2\sigma$ at 300K and 700K. RCPU is the relative CPU time per single SCF cycle [RCPU(TZ) ≡1].

Basis set	*a*(Å)	y	z	E	FL	E_g	q(Ca)	*x*		RCPU
								300K	700K	
TZ	9.2182	0.3339	0.1620	-682.979	-2.20	0.37	1.56	0.02	0.05	1.00
DZ1	9.2383	0.3339	0.1632	-682.874	-2.39	0.34	1.59	0.03	0.05	0.74
DZ1d	9.2423	0.3335	0.1615	-682.892	-2.50	0.36	1.55	0.02	0.05	0.75
DZ2	9.2348	0.3337	0.1618	-682.844	-2.88	0.32	1.55	0.03	0.05	0.35
DZ2d	9.2334	0.3329	0.1619	-682.871	-3.02	0.38	1.52	0.03	0.05	0.37

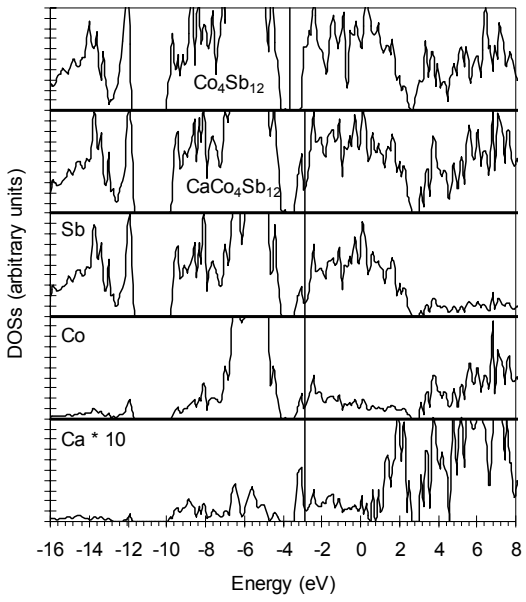

Figure 1. Total and atom projected DOS (B3PW91/DZ2). Except for Ca, the same scale is used for all DOS plots. Projected DOS are scaled by the number of contributing atoms. The vertical line indicates the Fermi level.

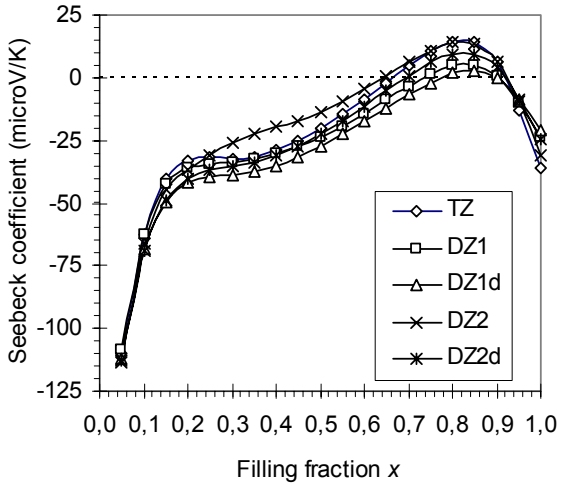

Figure 2. DFT B3PW91, calculated Seebeck coefficient at 300K as a function of the filling fraction *x* in the frozen band approach (*x*=1 band structure) with various basis sets (see text).

When Ca is placed in the *2a* position, it acts as an electron donor element. The Fermi level rises in energy, crossing the first three Co_4Sb_{12} conduction bands (bands 69-71). The Co_4Sb_{12} band gap becomes roughly halved in $CaCo_4Sb_{12}$ (E_g, table 2). Addition of Ca yields a *n*-doping level, P_e, of 2 e^- /formula unit with respect to the undoped Co_4Sb_{12}, as calculated by projecting the 1-density matrix into the energy interval between the FL of the filled system and the top of the valence band in Co_4Sb_{12}. The Ca atom gives a non negligible contribution only to the bands that either cross or lie above the FL, the highest contribution (0.21 e^-) being that to band 69 (former Co_4Sb_{12} FUB) and mainly due to the Ca 4*s* states [26]. A non-negligible overlap Mulliken's population is observed for Ca only with the nearest neighbors Sb atoms, due to the Ca 4*s* – Sb 5*p* interaction.

Upon insertion of a Ca atom, the cell parameter increases with respect to Co_4Sb_{12} and the Sb_4 ring becomes more squared, as revealed by a $2\cdot(y_{opt} + z_{opt})$ value much closer to one, y_{opt} and z_{opt} being the optimized free Sb coordinates [27]. This picture is found for all levels of theory considered in this paper. The optimized cell structures have low variability. Considering the TZ cell structure as the most accurate, the cell parameter increases by only 0.2% on+9 passing from TZ to DZ1 and a similar behaviour is observed for the DZ1d, DZ2 and DZ2d basis sets. In all cases, the two free fractional coordinates of Sb remain almost constant while varying the computation level.

The calculated cell parameters are all overestimated by about 1.2-1.4% with respect to an hypothetical value of 9.106Å obtained by linearly extrapolating the available experimental data for $CaCo_4Sb_{12}$ [7]. The atom and the shell projected DOS are almost unchanged with the basis sets. When a single *d* shell is added (DZ1d and DZ2d basis sets) for the Ca atom to the 2-ζ basis sets, the Ca *d* states lie either relatively far below or significantly far above the FL, and they can not thus contribute significantly to the ETPs, which crucially depend upon the shape of the bands just around the FL.

The E_g value slightly changes with the different basis sets, lying in the 0.32-0.38 eV range. This value plays a role in determining the ETPs for the low-doped binary skutterudites, using the frozen band approach. Indeed, the lower is E_g the higher turns out to be the contribution from bands lying just below the band gap region. Since these bands bring about positive contributions to the global S value, |S| is found to decrease with decreasing E_g. The trends of S at 300K, as a function of the *x* filling fraction (figure 2), show an high similarity for the various basis sets, as expected from the small changes observed for the corresponding electronic structures. The differences among the calculated best *x* filling fraction are almost negligible (table 2) and even more so for the higher temperature considered (700K). Interestingly, when the filling fraction is decreased to low values ($x<0.2$), only the 69th band contributes significantly to the ETPs. The band structure of the fully filled system ($CaCo_4Sb_{12}$) was used here in the frozen band approach. Similar small changes with basis sets were observed when the Co_4Sb_{12} system is taken as a reference, but experimental ETPs are badly reproduced in this case (see 3.2).

As a final remark of this paragraph, we observe that the DZ2 atomic basis set yields results of similar quality to those obtained with the TZ basis set, but with one third of the computational cost.

3.2. Frozen band approximation : supercell vs single cell approach

Supercell *vs* single cell electronic structure computations provide reference band structures of systems which have a filling fraction closer to reality than the fully filled $CaCo_4Sb_{12}$ system adopted in the previous paragraph, while not being zero as in the unfilled Co_4Sb_{12} system. The supercell approach has however the disadvantage of being highly computational demanding. Using a 2x1 supercell, the number of nuclei and electrons per unit cell is almost doubled and the number of symmetry operations reduced from 24 (x=1) to 4 (x=0.5). As a result, the CPU time increases by about two order of magnitude with respect to the single cell approach.

The trends of the calculated ETPs using two different reference band structures (1×1 $CaCo_4Sb_{12}$ and 2×1 $Ca_{0.5}Co_4Sb_{12}$) and two different levels of theory (B3PW91/DZ2 and LDA/DZ2) are shown in figure 3 (*left* and *middle* panels). For the sake of comparison, the results obtained using the unfilled 1×1 Co_4Sb_{12} band structure are also illustrated. The electronic structures of 1×1 $CaCo_4Sb_{12}$ and 2×1 $Ca_{0.5}Co_4Sb_{12}$ showed no significant differences and are not reported here.

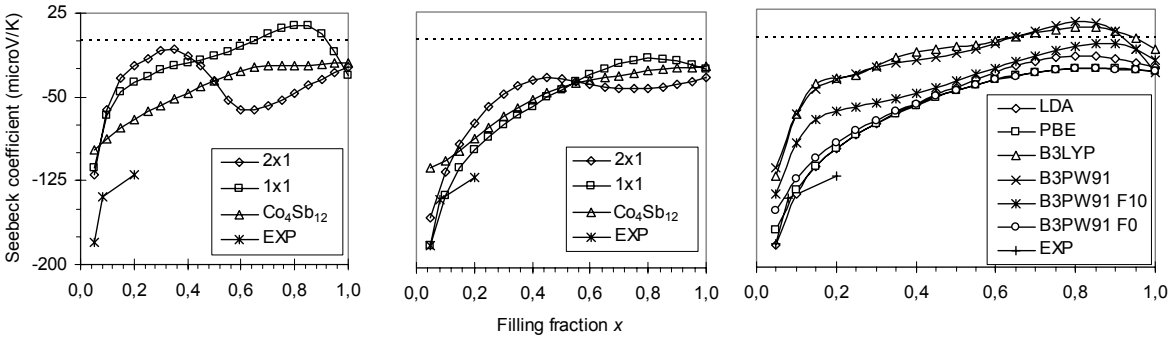

Figure 3. Calculated Seebeck coefficient at 300K as a function of the filling fraction *x*. DZ2/B3PW91 (*left*) and DZ2/LDA (*middle*) with different reference band structures; DZ2 basis set with different DFT functionals and *x*=1 band structure (*right*). Experimental values from [6].

From figure 3, it is clear that a good agreement on the computed S values and their slopes against *x*, is only observed between the reference models that take into account the band modifications due to the presence of Ca and only for *x* below 0.2-0.3. Such an agreement can be rationalized as follows. When *x* is low, the Fermi energy level becomes located close to the band gap zone and the bands giving the largest contributions to S are explicitly energy optimized for both the 1×1 $CaCo_4Sb_{12}$ and 2×1 $Ca_{0.5}Co_4Sb_{12}$ systems. These bands have non negligible contributions from the orbitals of the Ca atom, which acts as an electron donor in both systems. Given the observed similarity of the Ca projected DOS of the two systems in the region immediately below the Fermi level, one argues that such a similarity will also apply to their underlying band structures and in the same energy range. This eventually leads to similar S values for the two systems. In fact, at low *x* values, the only bands that appreciably contribute to the Seebeck coefficient are those located in this energy region. Conversely, when *x* is larger, the Fermi level is shifted upward in energy in regions where the bands of the 1×1 $CaCo_4Sb_{12}$ and 2×1 $Ca_{0.5}Co_4Sb_{12}$ systems largely differ since only those of the former are explicitly optimized. The S values calculated with the unfilled Co_4Sb_{12} system band structure as a reference are instead quite far from those obtained from the filled band structures, even for the low filling fractions.

3.3. DFT functional

Four DFT functionals, among those more commonly used for the modeling of TE materials, have been considered: Becke3 [16] exchange potential with PW91 [17] (B3PW91) or LYP [28] (B3LYP) correlation potential functionals; Perdew, Burke, and Ernzerhof [29] (PBE) exchange-correlation functional; local-density approximation [30] (LDA) functional. DZ2 basis set was adopted in all cases and the results are reported in table 3. All functionals found $CaCo_4Sb_{12}$ to be an heavily *n*-doped semiconductor with both total and atom projected DOS scarcely affected by the selected functional. The optimized cell parameters are all overestimated with respect to the extrapolated experimental value of 9.106Å, in a range that goes from +0.92% (LDA) to +2.8% (B3LYP) of such a value.

Table 3. $CaCo_4Sb_{12}$, DZ2 basis set: the effect of the DFT functional.

	a(Å)	y	z	FL	E_g	Q(Ca)	*x*		RCPU
							300K	700K	
B3PW91	9.2348	0.3337	0.1618	-2.88	0.32	1.55	0.03	0.05	2.99
B3LYP	9.3637	0.3340	0.1613	-2.67	0.20	1.53	0.02	0.05	2.36
PBE	9.3135	0.3338	0.1640	-3.05	0.20	1.55	0.10	0.20	2.38
LDA	9.1910	0.3320	0.1649	-2.91	0.37	1.50	0.10	0.15	1.00
B3PW91-F10	9.2364	0.3335	0.1618	-2.88	0.32	1.54	0.03	0.12	2.66
B3PW91-F0	9.3313	0.3335	0.1618	-3.07	0.17	1.55	0.10	0.20	2.10

Total and atom projected DOS for the various functionals look very similar to that shown in figure 1 and are thus not reported.

As for the trends of the Seebeck coefficient, two distinct groups of results are clearly recognizable in figure 3 (*right*), those for PBE and LDA and those for the B3PW91 and B3LYP hybrid functionals. These latter yield very similar S values, within few μV/K, with much lower |S| values with respect to LDA and PBE, particularly for the low filler fractions. The PBE and LDA functionals predict S values also close to each other, but in better agreement with experiment. One reason for this clustering of the calculated S values in two groups is related to the role played by the exact Hartree-Fock (HF) exchange in the Becke3 exchange part of the hybrid functionals. Indeed, if the percentage of the HF exchange is lowered from the original value of 20% down to 10% and 0% (B3PW91-F10 and B3PW91-F0 functionals), the |S| values increase and get progressively closer (figure 3, *right*) to the LDA and PBE ones. Finally the differences among LDA, PBE and B3PW91-F0 S values are in the order of few tenth of μV/K, with the greatest difference found at x = 0,05 (LDA = -180; PBE = -167; B3PW91-F0 = -150). The optimized filler fractions x (table 3) do not exceed the experimental value of x = 0.2, for any adopted functional. PBE and LDA give similar values, larger than those obtained from the hybrid functionals and very close to the experimental value of 0.2 obtained at 700K.

From the comparison of the obtained results, the PBE and LDA appear as the most reliable DFT functionals for the calculation of the ETPs of the $Ca_xCo_4Sb_{12}$ system. Furthermore, LDA gives better optimized cell parameters with a lower computational cost. However, it is worth mentioning that for the $Ba_xCo_4Sb_{12}$ system, the B3PW91 S values, for several filler fractions, are in general better agreement with experiment than the LDA ones. Due to the several aspects that can not be modeled (*e.g.* presence of substitutional disorder or of native defects) or that are drastically simplified (costant relaxation time) by the present *ab-initio* approach, agreement with experiment should be judged more by comparing trends, rather than absolute values of the ETPs. Keeping this in mind, the various DFT functionals we investigated can probably be considered to perform similarly (figure 3, *left*).

4. Filler's fraction and accuracy of the computed electron transport properties

The computation of ETPs from *ab-initio* determined band structures has been extensively tested for $CaCo_4Sb_{12}$. For low filling fraction values (up to x=0.2) the 1×1 and the 2×1 reference band structures give comparable results. Overall, we find that the 1×1 LDA/DZ2 DFT model leads to reasonable results, at a moderate computational cost. Using this model, the trends of the Seebeck coefficients are generally in good agreement with experiment, the computed values at 300K differing only within few per cent from the experimental values at x=0.05 and x=0.08 [6]. However, at the highest experimental filling fraction, x=0.2, a deviation of 24.2% is observed. This fact might be interpreted in two ways. On the one hand, as a failure of our model, which could either be inadequate for this intermediate filling fraction, or simply far from the real nature of the experimental sample where structural and compositional disorder is always necessarily present. On the other hand, it might be interpreted as a result of an experimentally overestimated filler's fraction. The experimental S value at x=0.2 is obtained only when x is halved and set equal to 0.1 in our computations. It is worth noting that we encountered a similar situation with $LaCo_4Sb_{12}$ [3]. At low filler's fractions the results from the band structure nicely agreed with experiment, whereas for x=0.23 the accord was very poor (-31.8 μV/K *vs* the experimental value of -80 μV/K). Using the $LaCo_4Sb_{12}$ band structure, only a filler's fraction halved to x=0.11 could return the experimental Seebeck value [3]. Our results for $R_xCo_4Sb_{12}$ (R= Ca, La) raise the important question of whether the Ca or La atoms have a far lower maximal solubility in Co_4Sb_{12} than claimed experimentally. Our doubt is further strengthened by observing that in the case of Ba filled systems, which are known to have an higher rattler's solubility (x=0.44)[31] with respect to R= Ca or La, the deviation of the computed S coefficients from experiment is not increasing with increasing filler's contents [3], but even slightly decreasing with x, despite a value of x as high as 0.44 is reached. We believe that this is a convincing argument in favour of suggesting the trend of the *ab-initio* computed Seebeck values as a possible diagnostic tool to assess how close to reality are the experimentally determined filler's fraction, and the more so the lower the filler's actual solubility is.

Acknowledgements
One of us (CG) wishes to express his warmest thanks to Prof. Cesare Pisani for his unmatched human kindness and for both the highlighting discussions had together and the precious scientific suggestions received from him through the years.

References

[1] Blake N P, Latturner S, Bryan D, Stucky G D and Metiu H 2001 *J. Chem. Phys.* **115** 8060
[2] Scheidemantel T J, Ambrosch-Draxl C, Thonhauser T, Badding J V and Sofo J O 2003 *Phys. Rev. B* **68** 125210
[3] Bertini L and Gatti C 2004 *J. Chem. Phys.* **121** 8983
[4] Madsen G K H, Schwarz K, Blaha P and Singh D J 2003 *Phys. Rev. B* **68** 125212
[5] Elliot S 1998 *The Physics and Chemistry of Solids* (New York: Wiley-Interscience)
[6] Puyet M, Lenoir B, Dauscher A, Dehmas M, Stiewe C and Muller E 2004 *J. Appl. Phys.* **95** 4852
[7] Puyet M, Lenoir B, Dauscher A, Weisbecker P and Clarke S J 2004 *J. Solid State Chem.* **177** 2138
[8] Saunders V R, Dovesi R, Roetti C, Orlando R, Zicovich-Wilson C M, Harrison N M, Doll K, Civalleri B, Bush I J, D'Arco Ph, Llunell M 2003 *CRYSTAL2003, User's Manual,* (Torino: University of Torino)
[9] Wadt W R and Hay P J 1985 *J. Chem. Phys.* **82** 284; Hay P J and Wadt W R 1985 *J. Chem. Phys.* **82** 299
[10] Bader R F W 1990 *Atoms in Molecules: a Quantum Theory* (Int. Ser. of monographs on chemistry **22**) (Oxford University Press)
[11] Gatti C 1999 *TOPOND-98: an electron density topological program for systems periodic in N (N=0-3) dimensions, User's Manual* (Milano: CNR-ISTM)
[12] Bertini L and Gatti C 2003 unpublished
[13] Saunders V R, Dovesi R, Roetti C, Causà M, Harrison N M, Orlando R and Zicovich-Wilson C M 1998 *CRYSTAL98, User's Manual* (Torino: University of Torino)
[14] The dependence of the calculated Seebeck coefficient on the number of points used to evaluate the integrals in equation (1) has been tested for $CaCo_4Sb_{12}$ at B3PW91/DZ2 level using increasingly finer grids (N^3 total points, with N ranging from 10 to 50). The resulting S values at 700 K, in μV/K, are : -37.6 (N=10), -50.9 (N=12), -50.5 (N=20), -54.1 (N=30), -55.2 (N=40) and –55.8 (N=50). The change in *S* is less than 1 μV/K on passing from N=30 to N=40 and about half of this from N=40 to N=50. Since the computational cost increases linearly with N^3, N=40 has been adopted
[15] Möllnitz L, Blake N P and Metiu H 2002 *J. Chem. Phys.* **117** 1302
[16] Becke A D 1993 *J. Chem. Phys.* **98** 5648
[17] Perdew J P and Wang Y 1989 *Phys. Rev. B* **40** 3399
[18] Ca, *s*: $\alpha = 0.035$, *p*: $\alpha = 0.0263$; Co, *s*: $\alpha = 0.0375$, *p*: $\alpha = 0.0230$
[19] Since the Ca 4p states lie at a very high energy with respect to the 4s, only one and two valence *p* basis functions for Ca were included in the DZ-like and in the TZ basis sets, respectively
[20] The outermost n*s* and n*p* gaussian functions were removed but retaining a double-ζ contraction scheme
[21] http://www.emsl.pnl.gov:2080/forms/basisform.html
[22] Anno H, Matsubara K, Caillat T and Fleurial J P 2000 *Phys. Rev. B* **62** 10737
[23] The local symmetry of Co is D_{3d}. In such a symmetry crystal field, with the z axis along the [1,1,1] direction, the *d* orbitals split into one A_{1g} and two degenerate E_g representations. The first is given by (*xy*+*xz*+*yz*) orbitals, while the second is an equally weighted combination of x^2-y^2 and z^2 orbitals
[24] Kurmaev E Z, Moewes A, Shein I R, Finkelstein L D, Ivanovskii A L and Anno H 2004 J. Phys. Condens. Matter **16** 979
[25] Partik M and Lutz H D 1999 *Phys. Chem. Minerals* **27** 41
[26] The 69-th band's Mulliken Population of the 4*s* orbital amounts to 0.17 e^-, which is about one order of magnitude higher than that of 4*p* (and of 3*d* orbitals, when present).
[27] According to the Oftedal's rule [Oftedal I 1928 Z. Kristallogr. A 66 517], the Sb_4 rings have exactly D_{4h} symmetry when $2\cdot(y+z)=1$, with *y* and *z* being the two free fractional coordinates of the Sb atom.
[28] Lee C, Yang W and Parr R G 1988 *Phys. Rev. B* **37** 785
[29] Perdew J P, Burke K and Ernzerhof M 1996 *Phys. Rev. Lett.* **77** 3865
[30] Vosko S H, Wilk L and Nusair M 1980 *Can. J. Phys.* **58** 1200
[31] Chen L D, Kawahara T, Tang X F, Goto T, Hirai T, Dyck J S, Chen W and Uher C 2001 *J. Appl. Phys.* **90** 1864